

N79-19034

Paper No. 25

**KINETICS DATA FOR DIFFUSION OF OUTGAS SPECIES  
FROM RTV 560**

C. K. Liu and A. P. M. Glassford, *Lockheed Palo Alto Research  
Laboratories, Palo Alto, California*

**ABSTRACT**

A detailed analytical and experimental study has been made of the outgassing behavior of RTV 560 silicone rubber. The four outgas species which predominate in the temperature range of 285 K to 425 K have been separately identified. The initial concentration of these species in the parent material and their bulk volatilities have been determined. The diffusion coefficients and activation energy for diffusion of the two major species have been deduced from outgassing rate data. It is shown that using these data in a diffusion theory model, the outgassing rates of these major species can be predicted for arbitrary geometry and any temperature within the range studied.

**INTRODUCTION**

To assess the possibility of contamination of critical spacecraft surfaces by condensation of outgas products from structural materials, it is necessary to have access to a data base for the outgassing behavior of these materials. In principle, this data base may take two forms. In the most common form, outgassing rates are measured experimentally for materials and components in the specific configurations and thermal environments which they will have and experience in practice. This type of data is cost effective and meaningful for given specific applications, but cannot be applied reliably to situations with different geometries and temperatures, for which additional measurements would be needed. A more fundamental approach is to identify the basic physical processes controlling the outgassing phenomenon, the physical relationships and equations representing these processes, and the basic physical properties of outgas species and parent material which relate to the controlling processes. When the basic physical properties have been measured experimentally, they can be used in conjunction with appropriate analytical solutions of the physical equations to predict outgassing rate for any desired combination of geometry and temperature history. This approach generates a universally applicable data base, and is clearly more suited to the assessment of contamination threats at the design stage. However, although the fundamental physical processes controlling outgassing are well understood qualitatively, it has not been possible in practice to obtain the necessary fundamental

physical properties. This is due in part to the difficulty of describing practical outgassing situations, where several species may be released simultaneously from a parent material by more than one mechanism - bulk diffusion, surface desorption, etc. It is also partly due to the lack of apparatus and experimental techniques sufficiently sensitive to generate data with enough resolution to permit separation of the various co-existing species and processes, and hence obtain fundamental property data.

This paper describes measurements in which some fundamental outgassing-related properties were obtained for RTV 560 silicone rubber, which is used extensively in the Shuttle Orbiter's Thermal Protection System. RTV 560 is prepared by mixing the uncured silicone with a catalyst. The principal outgas species from the cured material originate as by-products from the curing process and are therefore initially distributed evenly throughout the bulk material. Outgassing in vacuum occurs by diffusion of these products through the bulk material to the free surface, whence they evaporate. In this case, the outgas situation can be adequately described and modeled by diffusion theory, while the data needed to support the model are therefore the diffusion properties of each species.

To measure the outgassing rate with the sensitivity needed to resolve these diffusion properties, an apparatus based on the use of the quartz crystal microbalance (QCM) was developed. Basically, this apparatus achieves the desired resolution capability by in situ measurement of the outgassing rate directly by condensation of outgassed molecular flux on a cooled QCM surface, rather than by the less sensitive method of measuring a weight change of a few percent or less in the parent material before and after each test.

The validity of the data was tested by using it to predict outgassing of RTV 560 samples of widely differing geometry and temperature.

## APPROACH

### Diffusion Model

The phenomenon of transient diffusion of molecules of one species through a solid of different composition can be expressed by Fick's Second Law.

$$\frac{\partial C}{\partial t} = -D \nabla^2 C \quad (1)$$

where  $C$  is the concentration of the diffusing species in the medium, in mass per unit volume, and  $D$  is the diffusion coefficient.  $D$  is highly temperature dependent and is commonly expressed by the following relationship,

$$D = D_0 \exp(-E_d/RT) \quad (2)$$

where  $E_d$  is the activation energy for diffusion and  $D_0$  is a constant. For diffusion in polymers,  $D$  can also be concentration dependent

(Ref. 1). However, this dependence should be negligible for the dilute concentrations that apply in the outgassing situation. Also,  $E_d$  may vary with temperature, but prior knowledge of this dependence is not necessary to the present analysis, which is based on isothermal conditions.

Equation (1) can be solved for any selected boundary conditions to determine the concentration distribution as a function of location and time. Many of these solutions are given by Crank (Ref. 2). For the case of outgassing from RTV 560 or similarly prepared polymer, the initial concentration,  $C_0$ , of the outgas species in the material is uniform. When the material is exposed to the vacuum environment, the concentration of these species at the free surfaces is reduced to a very low value by evaporation. If the internal diffusive flow resistance is high compared with the effective surface evaporation "flow resistance," then it can be assumed that the outgas species concentration is zero at the free surface. In practice, a material cannot be instantaneously exposed to the vacuum environment, since a minimum of several minutes are required to evacuate the test chamber to low pressure. However, this period is very short compared with the total exposure time for tests lasting periods of days, and hence the pressure reduction can be considered to be essentially instantaneous. The boundary conditions to the diffusion equation applicable to the outgassing situation are thus

$$\text{at } t = 0, C (\text{throughout}) = C_0$$

$$\text{at } t > 0, C (\text{free surface}) = 0$$

For most practical outgassing situations and in the tests reported in this paper, the diffusive flow is approximately one dimensional in rectangular coordinates. This situation is shown in Figure 1 for flow from both sides of an infinite slab of thickness,  $L$ . Since there is a no-flow boundary at  $x = L/2$ , this model also applies to outgassing from one side of a slab of width  $L/2$  whose other side is sealed. For this case, Eq. (1) becomes

$$\frac{\partial C}{\partial t} = -D \frac{\partial^2 C}{\partial x^2} \quad (3)$$

while the boundary conditions are

$$C(x, 0) = C_0$$

$$C(0, t) = C(L, t) = 0$$

The solution to Eq. (3) with these boundary conditions (Ref. 3) is

$$C(x, t) = \frac{4C_0}{\pi} \sum_{m=0}^{\infty} \frac{1}{2m+1} \cdot \sin \frac{(2m+1)\pi x}{L} \exp \left[ -\frac{D(2m+1)^2 \pi^2 t}{L^2} \right] \quad (4)$$

The outgassing rate,  $\dot{Q}$ , in mass per unit area per unit time leaving the free surface is equal to the concentration gradient at the surface multiplied by the diffusion coefficient,

$$\dot{Q} = D \left| \left( \frac{\partial C}{\partial x} \right)_{x=0, L} \right| \quad (5)$$

From Eqs. (4) and (5),

$$\dot{Q} = \frac{4DC_0}{L} \cdot \sum_{m=0}^{\infty} \exp \left( \frac{-D(2m+1)^2 \pi^2 t}{L^2} \right) \quad (6)$$

$$\frac{\dot{Q}L}{DC_0} = 4 \sum_{m=0}^{\infty} \exp \left( \frac{-D(2m+1)^2 \pi^2 t}{L^2} \right) \quad (7)$$

The nondimensional outgassing rate,  $\dot{Q}L/DC_0$ , is plotted versus nondimensional time,  $Dt/L^2$  in Figure 2. From the log-log plot it can be seen that  $(\dot{Q}L/DC_0)$  varies as  $(Dt/L^2)^{-1/2}$  for times less than  $0.03 L^2/D$ . From the log-linear plot, it is seen that for times greater than  $0.06 L^2/D$ ,  $(\dot{Q}L/DC_0)$  varies exponentially with time. This is due to the fact that all terms in Eq. (7) for  $m \geq 1$  become negligible by comparison with that for  $m = 0$ . Therefore, Eq. (6) can be rewritten as

$$\dot{Q} = \frac{4DC_0}{L} \exp \left[ -\left( \frac{D\pi^2}{L^2} \right) t \right], \quad t > \frac{0.06 L^2}{D} \quad (8)$$

Hence, if experimental isothermal (i.e., constant  $D$ ) outgassing data for time greater than  $0.06 L^2/D$  are plotted versus time on a log-linear plot, a straight line of slope  $(-D\pi^2/L^2)$  and intercept  $(4DC_0/L)$  should be obtained, from which  $D$  and  $C_0$  can be calculated.

#### Species Identification

For the case of outgassing from polymers, there will be in general, several species diffusing through the parent material simultaneously.

An essential feature of the experimental apparatus required to determine  $D$  and  $C_0$  is therefore a means to identify each outgas species. In the present work the means used was to measure the bulk evaporation rates of the different species. The experiment to perform this measurement will be described in Species Identification Experiments. The relevant theory is based on a modified Langmuir equation,

$$\frac{\dot{m}_e}{A} = \alpha_e P_v \sqrt{\frac{M}{2\pi RT}} \quad (9)$$

Here  $(\dot{m}_e/A)$  is the measured evaporation rate per unit area,  $P_v$  is the vapor pressure of the species,  $M$  is its molecular weight, and  $T$  is the temperature.  $\alpha_e$  is an empirical evaporation coefficient, less than or equal to unity, which accounts for nonideal behavior at high evaporation rates, less than total surface coverage, etc. The vapor pressure of most substances can be approximated by an equation with the following form

$$\ln P_v = B_1 - H_L/RT \quad (10)$$

where  $H_L$  is the latent heat of vaporization and  $B_1$  is a constant. Combining Eqs. (9) and (10) gives

$$\ln \frac{\dot{m}_e}{A} \sqrt{T} = B_2 - H_L/RT \quad (11)$$

where

$$B_2 = B_1 + \ln \left( \alpha_e \sqrt{\frac{M}{2\pi R}} \right) \quad (12)$$

Hence, if the evaporation rate of an outgas species is measured as a function of temperature, a plot of  $\ln (\dot{m}_e/A \cdot \sqrt{T})$  versus  $1/T$  should be linear with a slope of  $(-H_L/R)$  and intercept of  $B_2$ . In general, different outgas species have different values of  $B_2$  and  $H_L$ , and will therefore have unique and distinguishable reevaporation characteristics.

## THE THERMAL ANALYSIS APPARATUS

### Apparatus Description

Experimental outgassing rate measurements were made by using the Thermal Analysis Apparatus (TAA), shown in Figure 3. The principal components of the TAA are a sample pot, a collector QCM, and a system of shrouds, all of which are thermally grounded to a liquid nitrogen reservoir. The sample pot is a cylindrical container with a small orifice in one end. The base of the sample pot contains an electrical resistance heater and a platinum resistance thermometer. By balancing the heat input to the sample pot against the heat leak along the sample pot support strut to the cooled shielding structure, the pot temperature can be controlled to any temperature above  $\sim 100$  K. A collector QCM is positioned along the normal line-of-sight of the sample pot orifice.

This QCM is normally allowed to cool to about 90 K, at which temperature all significant outgas species impinging on its surface will be condensed. The QCM views the sample pot orifice through a shuttered hole in the shielding structure, permitting the impinging flux to be interrupted when appropriate. Both QCM and sample pot are completely surrounded by the cooled shrouding to reduce the background outgassing rate to undetectably low levels.

The QCM is mounted in an aluminum holder with an electric resistance heater. Its temperature can be controlled to any temperature between about 90 K and 420 K by balancing electrical heat input against heat leakage along its support struts to the liquid nitrogen reservoir. The QCM is a Celesco Model 700 unit, which contains a built-in platinum resistance thermometer. The accuracy of this QCM has been established in a previous work (Ref. 4).

The material sample being tested is held within the sample pot in a holder configured to produce one-dimensional diffusive flow during outgassing. Sample preparation and holder geometry will be described in Sample Preparation.

#### Experimental Procedure

The general experimental procedure used in the TAA was as follows:

(1) After weighing and installing the sample and holder in the sample pot, the apparatus was assembled, the bell jar was replaced, and the system evacuated. About 5 minutes after the beginning of evacuation, the pressure was low enough to switch to the diffusion pump and to fill the liquid nitrogen pot. The final pressure was below  $2 \times 10^{-7}$  torr, measured outside the cold shroud.

(2) Thermal equilibrium was attained in the second phase of the tests. The QCM cooled down to near 90 K in about 1 hour. The sample pot was either heated electrically or allowed to cool to reach the particular test temperature selected. This took from 1/2 to 2 hours, depending upon the required temperature difference from ambient.

(3) The outgassing rate was measured by opening the shutter and collecting the outgas flux on the QCM. The QCM reading was recorded as a function of time. The measurement began as soon as the system pressure fell below about  $10^{-5}$  torr. However, not all of the impinging flux would condense on the QCM until it was quite cold, and since the QCM output is temperature dependent, the data were difficult to resolve until thermal equilibrium was approached. However, steady state measurements with equilibrated QCM and isothermal sample could be obtained within about 1 hour of beginning the evacuation.

(4) When the QCM had accumulated a substantial deposit, or at any other arbitrarily specified time, the shutter was closed and the QCM heated slowly, while the reevaporation rate of the collected outgassing species was recorded as the crystal cleaned up.

(5) Experiments were terminated when the outgassing rate data had become linear on a log-linear rate versus time plot. This usually took 1 to 7 days. The apparatus was then warmed up, let back to atmosphere with laboratory air, and the sample removed and reweighed.

### Data Reduction Procedure

The measured data were QCM frequency outputs; time since initiation of an experiment; sample pot and QCM temperatures; and sample initial and final weight, measured at 1-atmosphere pressure. Reduction of all of these data except QCM frequency is straightforward. The deposit mass per unit area on the QCM crystal is equal to the frequency shift from the clean condition multiplied by the QCM sensitivity constant,  $4.43 \times 10^{-9}$  gms/cm<sup>2</sup>/Hz. The mass collection rate per unit area on the QCM was obtained from the deposit mass per unit area versus time data. The total mass flow rate through the sample pot orifice,  $\dot{m}_o$ , is related to the QCM mass collection rate per unit area,  $(\dot{m}/A)_q$ , as follows

$$\frac{\dot{m}_o}{\pi r^2} = \left(\frac{\dot{m}}{A}\right)_q \times 0.98 \quad (13)$$

where  $r$  is the distance from the sample pot orifice to the QCM crystal surface and the factor 0.98 is an empirical factor allowing for the fact that the flux distribution from the orifice is not a pure cosine function because of the finite thickness of the orifice. This factor was determined by scanning the flux distribution from a similar orifice in an earlier experiment. The outgassing rate from the sample in the pot is equal to  $\dot{m}_o$  divided by the exposed sample area.

For the case of evaporation of the deposit from the QCM surface during warmup, the measured rate of deposit mass loss is less than the true evaporation rate due to the finite flow resistance of the aperture in the QCM casing. The true evaporation rate is equal to the measured rate divided by 0.805 (Ref. 4).

### OUTGASSING EXPERIMENTS

#### Sample Preparation

Material Preparation - The material selected for the outgassing tests was RTV 560, a two-component room temperature vulcanizing (RTV) silicone rubber produced by the General Electric Company (Ref. 5). RTV 560 is a methyl-phenyl compound which will be used extensively as an adhesive in the Space Shuttle Orbiter Thermal Protection System. This material was prepared in the laboratory in 40-gram batches. Two drops of dibutyl tin dilaurate catalyst were used for 40 grams of silicone which, according to the manufacturers data, corresponds to 0.1% by weight. The low catalyst percentage was selected for these tests to extend the curing time and give entrapped air more time to escape. Although the size of a drop is not a standardized quantity, this procedure gave approximately the same curing time as predicted by the manufacturer as well as good batch-to-batch data agreement.

Sample Holder - The basic type of sample holder used is shown in Figure 4a. It is made from stainless steel in the form of a flat disk,

2.85-cm diameter, and 0.51-cm thick, with a cylindrical recess of 2.29-cm diameter and 0.25-cm deep. The recess was totally or partially filled with RTV 560, which was then cured in place, forming a disk-like sample. The holder geometry constrains the outgassing flow to be one-dimensional, perpendicular to the free surface of the sample. (In this case,  $L$  is equal to twice the sample thickness, since outgassing takes place from only one side of the sample.) The sample holder dimensions were selected in accordance with two criteria. The total amount of material had to be adequate to provide a measurable deposit mass flux at the QCM surface, but could not be so high as to exceed the capacity of the QCM. Also, since  $D$  and  $C_0$  are extracted from outgassing data for evacuation times greater than  $0.06 L^2/D$ ,  $L$  had to be small enough to prevent this minimum time from being excessive. Since neither  $D$  nor the outgassing rates were known in advance, these dimensions had to be estimated. However, the dimensions given proved to be adequate for most of the sample temperature range investigated.

A second type of holder, shown in Figure 4b, was used in later experiments in which the object was to investigate the validity of the diffusion theory and the generated data when applied to the outgassing of RTV 560 at large  $L$ . These holders were made from stainless steel tubing of 0.48- to 0.88-cm inside diameter and had an effective  $L$  of the order of 2.1 to 2.4 cm. (In this case,  $L$  is equal to the holder length, since outgassing takes place from both ends.) As with the disk-type holders, the sample was cured in place.

Sample Storage — It was noted during the early experiments that the proportion of the most volatile of the outgas species decreased noticeably with time if the samples were stored at room temperature before vacuum exposure. To reduce this effect, later samples were stored in a refrigerator between the end of curing and the beginning of vacuum testing.

#### Species Identification Experiments

Before attempting to measure  $D$  and  $C_0$  for each outgas species, it was necessary to establish a technique for identifying them individually. In the present work this was done by means of their evaporation characteristics, as was described earlier. A preliminary series of tests was conducted in which a sample of RTV 560 was heated until a significant deposit had accumulated on the cooled QCM. After interrupting the impinging flux, the QCM was heated slowly and the QCM output was measured as a function of temperature. Typical warmup data are presented in Figure 5, showing the successive evaporation of three different species. The evaporation rate,  $\dot{m}_e/A$ , can be calculated as a function of temperature,  $T$ , from the rate of change of the QCM output during warmup. When these rates are plotted as  $\ln(\dot{m}_e/A \cdot \sqrt{T})$  versus  $1/T$ , several distinct linear characteristics are obtained, each corresponding to a separate outgas species as discussed in Approach. For the temperature range of 10°C to 150°C, four species were found and referred to as  $M_1$ ,  $M_2$ ,  $M_3$ , and  $M_4$ , in order of increasing

volatility. The characteristics in Figures 5 and 6 were reproducible from test to test, and served as a reliable means for identifying the proportions of each species collected on the QCM at any point in the later isothermal outgassing tests.

According to Eq. (11), it should be possible to deduce the latent heat of the various species from the slopes of the respective reevaporation characteristics. However, these characteristics are plotted from apparent reevaporation rate data, as indicated by the QCM. It is known that the response of the QCM to liquid deposits is less than 100% and becomes less as the temperature increases due to the decrease of viscosity in the liquid deposit (Ref. 6). The indicated loss of QCM output for evaporating liquid deposits will therefore be due partly to actual evaporation, and partly to loss of QCM sensitivity. During many of the QCM warmup experiments, a sudden increase in the apparent evaporation rate was frequently observed, which always occurred at the same temperature for a given outgas species. This discontinuity was interpreted as being due to a loss of QCM response as the deposit changed phase from solid to liquid. The outgas species property data that can be reliably extracted from the QCM warmup measurements are thus heat of sublimation for the solid phase, and the melting point of each species. These are shown in Table 1. For the portion of the warmup curve of each species at temperatures above its melting point, the apparent evaporation rates will be erroneously high, making the slopes of the data meaningless. However, the fractional loss of QCM response due to viscous effects is a function of viscosity and true deposit mass per unit area (Ref. 6). In most of the tests, the QCM warmup measurements were begun with about the same mass on the crystal (approximately  $8 \times 10^{-5}$  g/cm<sup>2</sup>). Since both viscosity and evaporation rates are functions of temperature, the indicated evaporation rates for the condensed species in the liquid phase were reproducible from test to test, permitting warmup data to be used for species identification. It is noted that this is a fortuitous situation, permitting positive species identification to be made in a specific apparatus. However, comparison of data for liquid phase evaporation from different workers should be made with extreme caution. Further development of QCM thermogravimetric technique is needed in this area.

Table 1. OUTGAS SPECIES OF RTV 560

Outgas Species	Melting Point (K)	Heat of Sublimation (K cal/g-mol)	Initial Concentration (g/cm <sup>3</sup> )	Activation Energy for Diffusion (K cal/g-mol)
M <sub>1</sub>	205	5.22 (200 K)	0.0084 (± 50%)	
M <sub>2</sub>	275	13.7 (260 K)	0.0456 (± 10%)	7.91
M <sub>3</sub>	319	8.62 (312 K)	0.0146 (± 10%)	8.49
M <sub>4</sub>	367	21.4 (362 K)	0.0056 (± 50%)	

### Isothermal Outgassing Tests

Test Program - A series of experiments was conducted in which the isothermal outgassing rates of RTV 560 samples was measured as a function of time. The tests and conditions are listed in Table 2. The primary object of these tests was to generate data from which  $D(T)$  and  $C_0$  could be deduced for each species. Most of the tests were conducted according to the general procedure described in Experimental Procedure. The exceptions are that in Tests 5, 6, and 7, the QCM was maintained at higher temperatures in order to collect only the less volatile species. The major portion of the diffusion coefficient data was obtained from Tests 3 through 8. Tests 4L, 9, and 10 were conducted primarily as part of the model verification, see Discussion. Test 8R was a repeat of Test 8 with a longer orifice to QCM line-of-sight distance,  $r$ , in which the  $1/r^2$  relationship assumed in the data reduction was successfully verified. (All tests were conducted at  $r = 10.09$  cm except Tests 8, 9, and 10 where  $r = 7.17$  cm.)

Although four species were identified in the overall test program, the major portion of the observed outgassing rate, and hence the derived diffusion coefficient data, related to species  $M_2$  and  $M_3$ . Species  $M_1$  is quite volatile and difficult to study without making special sample holders with very long diffusion paths and/or storing in a refrigerator before the test, so as to delay the outgassing process sufficiently for it to be studied. In practical applications where the cured RTV 560 is stored at room temperature,  $M_1$  will outgas completely in a very short time and will not pose a problem. Since its volatility is high, it is also less likely to condense on a critical surface. Hence, no concerted attempt was made to study the diffusion of  $M_1$  in detail.  $M_4$  was encountered only at the higher end of the temperature range studied, and data obtained were not sufficient for determination of  $D$  as a function of temperature. However, there is every reason to believe that extension of the test program to higher temperatures would enable  $M_4$  to be characterized in a manner similar to  $M_2$  and  $M_3$ .

Data Analysis - The isothermal outgassing rate versus time data for all tests were basically similar in form. As a typical example, data for Test 8 is shown in Figure 7. In Test 8, species  $M_2$  predominated in the early stages while  $M_3$  predominated at later times. The slope of the linear portion of the  $M_3$  data at these later times is quite clear and  $D_3$  can be determined with confidence. At early times, however, the slope of the linear portion of the  $M_2$  data is less obvious and difficult to interpret. Hence, in those tests where more than one species was found, usually only the later portion of the curves was used to obtain slope data. By plotting the isothermal outgassing data from the tests of Table 1 in the manner of Figure 7, it was possible to obtain  $D$  for species  $M_2$  and  $M_3$  for a number of temperatures. Noting Eq. (2), these data for  $D_2$  and  $D_3$  have been plotted in Figure 8 in the form  $\ln D$  versus  $1/\text{temperature}$ . Linear relationships are obtained for both species which can be fitted by the following equations.

$$D_2 = 0.03324 \exp(-7910/RT) \quad (14)$$

ORIGINAL PAGE IS  
OF POOR QUALITY

Table 2. RTV-560 OUTGAS TEST SUMMARY

Test No.	Sample Temperature (K)	OCM Temperature (K)	Diffusion Length (L, cm)	Sample Weight (gms)	Total Weight Loss (%)	Test Duration (hr)	Outgas Species Observed	Diffusion Coefficient (D, cm <sup>2</sup> /S)
1	408.0	100	0.50	1.4728	2.66	28	M <sub>2</sub> , M <sub>3</sub>	D <sub>2</sub> = 1.47 × 10 <sup>-6</sup>
2	305.5	100	0.47	1.3817	1.53	147	M <sub>2</sub>	D <sub>2</sub> = 7.58 × 10 <sup>-8</sup>
3	343.5	100	0.47	1.3711	2.34	.21	M <sub>2</sub> , M <sub>3</sub>	D <sub>2</sub> = 3.12 × 10 <sup>-7</sup> D <sub>3</sub> = 2.65 × 10 <sup>-8</sup>
4	383.0	100	0.40	1.1744	3.01	101	M <sub>2</sub> , M <sub>3</sub>	D <sub>2</sub> = 1.01 × 10 <sup>-6</sup> D <sub>3</sub> = 7.94 × 10 <sup>-8</sup>
5	422.0	264	0.38	1.1394	3.64	52	M <sub>2</sub> , M <sub>3</sub> , M <sub>4</sub>	D <sub>2</sub> = 2.94 × 10 <sup>-6</sup> D <sub>3</sub> = 2.76 × 10 <sup>-7</sup>
6	423.0	300	0.56	1.6651	3.16	26	M <sub>3</sub> , M <sub>4</sub>	D <sub>4</sub> = 3.30 × 10 <sup>-7</sup>
7	423.0	340	0.52	1.5533	3.23	32	M <sub>4</sub>	D <sub>2</sub> = 1.05 × 10 <sup>-6</sup>
4L	383.0	100	2.42	0.6308	2.08	127	M <sub>2</sub> , M <sub>3</sub>	D <sub>2</sub> = 1.58 × 10 <sup>-6</sup>
8	398.0	100	0.25	0.7473	2.88	25	M <sub>2</sub> , M <sub>3</sub>	D <sub>3</sub> = 1.39 × 10 <sup>-7</sup>
8R	398.0	100	0.22	0.6588	3.17	49	M <sub>1</sub> , M <sub>2</sub> , M <sub>3</sub>	D <sub>1</sub> = 9.0 × 10 <sup>-6</sup> D <sub>2</sub> = 1.33 × 10 <sup>-6</sup> D <sub>3</sub> = 1.18 × 10 <sup>-7</sup>
9	298.0	90	2.07	1.7809	0.49	96	M <sub>1</sub> , M <sub>2</sub>	D <sub>1</sub> = 3.24 × 10 <sup>-6</sup>
10	284.5	90	2.05	1.7559	0.26	71	M <sub>1</sub> , M <sub>2</sub>	D <sub>1</sub> = 3.03 × 10 <sup>-6</sup>

$$L_3 = 0.006316 \exp(-8490/RT) \quad (15)$$

The activation energies for diffusion,  $E_d$ , for  $M_2$  and  $M_3$ , are thus 7910 and 8490 cal/mol, respectively.

In principle,  $C_0$  can be obtained from the intercept of the linear portion of the  $\ln Q$  versus time curve, as noted in the section on Diffusion Model. However, a systematic error is present in this intercept when drawn from experimental data, due to the finite time required to evacuate the apparatus and to heat the sample to equilibrium test temperature. These effects tend to displace the experimental data in Figure 7 to the right, which, in turn, leads to a larger apparent value for the intercept. This displacement can be partially corrected for, but some error is inevitable. Furthermore, small random errors in determining the slope are magnified into large random errors in intercept reading because of the logarithmic nature of the ordinate. The net effect of these influences is to attach relatively large uncertainty bounds to the  $C_0$  value deduced from the intercept.

The value of  $C_0$  can also be estimated from weight loss measurements, since for relatively long evacuation periods  $C_0$  will be only slightly higher than the total mass loss. In the present apparatus, the weight loss measurements were made *ex situ*, in which the raising of the local pressure to 1 atmosphere introduced an unknown error. Also, when more than one species are being outgassed, it is difficult to resolve the relative amounts of each species.

The value of  $C_0$  can also be calculated from the total amount collected on the QCM during an experiment, while the relative proportions of each species can be found from QCM warmup data of the type shown in Figure 5. Since the QCM measurements were made *in situ*, they are inherently more reliable than the *ex situ* weighings. However, the loss of QCM response when the deposit melts and the fact that more than one QCM warmup had to be made per test introduces new sources of uncertainty.

The most satisfactory method for obtaining reliable and consistent values of  $C_0$  was by selecting the values which gave the best correlation between experiment and theory for all tests. This was possible only for species  $M_2$  and  $M_3$  because of the lack of sufficient detailed experimental data for  $M_1$  and  $M_4$ . The theoretical predictions were made as described in the following section. The values for  $C_{O2}$  and  $C_{O3}$ , selected by this method and estimated to be accurate to  $\pm 10\%$ , are given in Table 1. Values of  $C_{O1}$  and  $C_{O4}$  estimated to a lower degree of certainty using the intercept and mass loss approaches are also given in Table 1.

These  $C_0$  data can be compared with Total Mass Loss (TML) and Volatile Condensable Material (VCM) data obtained from SRI-type tests for samples outgassed at 125°C for 24 hours. For RTV 560 with regular curing, Ref. 7 gives a TML of 0.0253 gms/gm. The Total Mass Available (TMA) for outgassing at 125°C is equal to the sum of the  $C_0$ 's (excluding  $C_{O4}$ , since no measurable amount of  $M_4$  was outgassed at 125°C), divided by the density of RTV 560 of 1.42 gms/cm<sup>3</sup>. This gives a TMA of 0.0483 gms/gm for the four components detected. The TML

should always be less than the TMA, although it should tend toward it for long evacuation periods. The TMA and TML from these two sources are therefore of the same order and do have the correct relationship. Further comparison of these data would require more knowledge of the sample size, preparation technique, and temperature history for which the TMA data were obtained. Reference 7 also gives the VCM at 298 K to be 0.0055 gms/gm. This would correspond to  $M_3$  alone,  $M_1$  and  $M_2$  being excessively volatile at 298 K. For  $M_3$  alone the TMA is 0.0103 gms/gm which is significantly higher than the VCM. However, this is to be expected, since  $M_3$  diffuses more slowly from the sample than  $M_1$  and  $M_2$ , and hence a lower fraction has outgassed in the 24-hour VCM test period.

#### Verification of the Data

With the data generated for  $D_2$ ,  $D_3$ ,  $C_{O_2}$ , and  $C_{O_3}$ , it is possible to predict the outgassing rates of  $M_2$  and  $M_3$  for an RTV 560 specimen of any geometry and temperature. Also, since  $M_2$  and  $M_3$  are the only significant species for the major part of the temperature range studied, the total outgassing rate,  $\dot{Q}_T$ , should be essentially equal to the sum of the rates for  $M_2$  and  $M_3$  i.e.,  $(\dot{Q}_2 + \dot{Q}_3)$ . To assess the accuracy with which the measured total outgassing rate could be predicted by  $(\dot{Q}_2 + \dot{Q}_3)$ , a comparison between measured and predicted data was made for four cases.

The measured data from Tests 4, 4L, 9, and 10 were used in the comparison. Tests 4 and 4L were both conducted at 383 K, but the flow path was about six times larger in Test 4L than in Test 4. These two tests, therefore, determine the effect of variable flow path length. Tests 9 and 10 were conducted for samples of length similar to Test 4L, but at temperatures of 298 K and 284.5 K. These two tests plus Test 4L reflect the effect of temperature variation over the range studied.

Since in each of these four cases the flow was one-dimensional, the outgassing rates for  $M_2$  and  $M_3$  can be calculated from Eq. (6), using diffusion coefficient data from Eqs. (14) and (15), and initial concentration data given in Table 1. It was assumed that diffusion of the two species proceeds independently, so the total outgassing rate is equal to the algebraic sum of the component rates. This calculation was made by computer for each of the temperature and length combinations corresponding to Tests 4, 4L, 9, and 10 given in Table 2.

The total outgassing rate data for Tests 4L and 4 and the predictions of  $(\dot{Q}_2 + \dot{Q}_3)$  for these tests are shown in Figure 9. It can be seen that the prediction agrees with the data to better than 10%. The predicted rates for  $\dot{Q}_2$  and  $\dot{Q}_3$  are also shown separately in Figure 9. For Test 4, most of  $M_2$  has been removed by 30 hours, after which the outgas species is almost totally  $M_3$ . With the increased diffusion path length of Test 4L, the main outgas species remains  $M_2$  for the entire duration of the experiment.

Figure 10 shows the total outgassing rate data and the predicted  $(\dot{Q}_2 + \dot{Q}_3)$  rates for Tests 9 and 10, at 298 K and 284.5 K, respectively. The agreement is not quite as good as at 383 K, but is still of the acceptable order of 10%. Since the agreement is better at 284.5 K than at

298 K, it is concluded that there is no systematic temperature dependent error, which in turn, means that the expressions for  $D_2$  and  $D_3$  in Eqs. (14) and (15) are accurate over the temperature range studied. The disagreement appears to be random, and is probably due to sample-to-sample variations in  $C_{O_2}$  and  $C_{O_3}$ .

## DISCUSSION

Within the range of temperature and geometric parameters studied, the goal of obtaining diffusion property data for the major outgas components of RTV 560 has been achieved. The validity of the data and the diffusion theory model has been verified in the parameter ranges studied by comparison of theoretical prediction and experimental data for several specific combinations, temperature, and geometry. In addition, the diffusion data generated and the technique of QCM thermogravimetry used to separate the different outgas species gives information on their relative volatility, which is often more useful than the outgassing data itself. For example, the data indicate that species  $M_2$  from RTV 560 will not condense on a 298 K surface with the normal level of impingement rates and hence, a detailed knowledge of the outgassing rate of  $M_2$  is not necessary if the surface of interest is at 298 K or higher.

Although the conclusions drawn from the present experiments must necessarily be confined to the parameter range studied, the analytical and experimental approach can be extended to a much broader parameter range for RTV 560, and also to many other polymeric materials in which the outgas products are originally bulk-distributed. Because of the greater amount of information provided by these experiments than by the usual engineering tests, the time and expenditure required for their performance is somewhat higher. Hence, it would be quite costly to generate diffusion data for the very large number of polymeric materials used in the aerospace industry. The most cost-effective use of the described techniques is to perform detailed outgassing analyses of those materials which constitute the most significant and/or commonly encountered outgassing sources, in terms of total amount of base material per spacecraft, percentage of outgassable material, and frequency of use on space vehicles. The detailed data would also be of great help in justifying or eliminating the need to high-cost, aerospace-grade materials in place of low-cost, commercial-grade materials.

In addition to the overall results of the experiments, two significant intermediate conclusions implicit in the final result should be emphasized individually.

First, the outgas products from RTV 560 consist of a small number of distinct species, whose properties and concentrations are reproducible between sample batches. Although no detailed study was made of the effect of catalyst percentage, it was observed by the authors in earlier tests on RTV 560 that increasing the catalyst percentage to 0.5% increased the initial concentrations of the outgas species, but did not alter their properties.

Second, the technique of using QCM thermogravimetry to differentiate between outgas species worked well. Since the QCM is the basic contamination sensor used in the aerospace industry, extension of its overall capability in contamination analysis is highly desirable.

However, although the volatility data obtained with a specific QCM in a specific application were repeatable, the absolute accuracy of the measured re-evaporation rate data generated is subject to error if the deposit is liquid, because of the degradation of QCM response in this case. Also, since the evaporation rate is highly temperature dependent, errors in measuring the true temperature of the evaporating deposit could complicate correlation of data from different experiments. Finally, the measured apparent evaporation rate of a real deposit expressed on a per unit substrate area basis may be less than the bulk evaporation rate, because it may be distributed in islands or droplets, instead of a uniform film. The area coverage factor then becomes another experimental parameter which can vary from application to application. In view of these factors, further development of QCM thermogravimetry is required to improve its quantitative capability.

#### ACKNOWLEDGMENTS

This work was performed as part of an Independent Research Program at the Lockheed Palo Alto Research Laboratory.

#### REFERENCES

1. Smith, T. G., "Review of Diffusion in Polymer Penetrant Systems," University of Maryland, NASA Contract No. NGR20-002-053, Sep 1968, p. 105
2. Crank, J., The Mathematics of Diffusion, Oxford University Press, London (1956)
3. Barrer, R. M., Diffusion in and Through Solids, Cambridge University Press, 1951
4. Glassford, A.P.M., "An Analysis of the Accuracy of a Commercial Quartz Crystal Balance," Paper No. 76-438, 11th AIAA-Thermophysics Conference, San Diego, Jul 1976
5. General Electric Company, Technical Data Book, S-35
6. Glassford, A.P.M., "The Response of a Quartz Crystal Microbalance to a Liquid Deposit," to be presented at 9th IES-AIAA-ASTM-NASA Space Simulation Conference, Los Angeles, Apr 1977
7. Campbell, W. A., Marriott, R. S., and Park, J. J., "A Compilation of Outgassing Data for Spacecraft Materials," NASA TN D-7362, NASA/Goddard Space Flight Center, Sep 1975

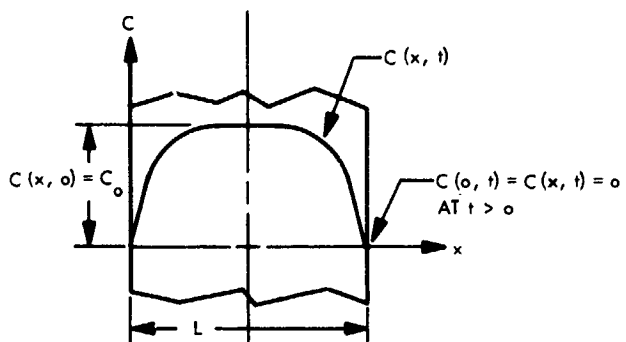


Fig. 1 Bulk Diffusion Model

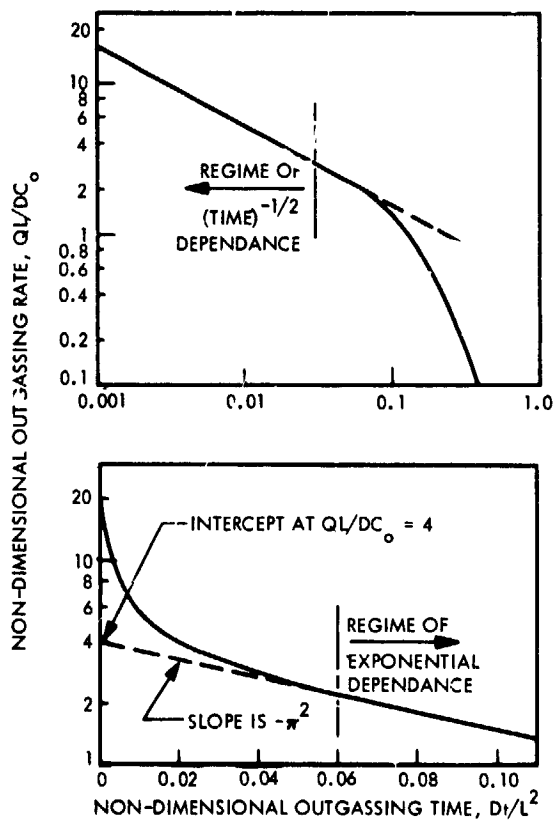


Fig. 2 Nondimensional Outgassing Rate

CRITICAL PAGE IS  
OF POOR QUALITY

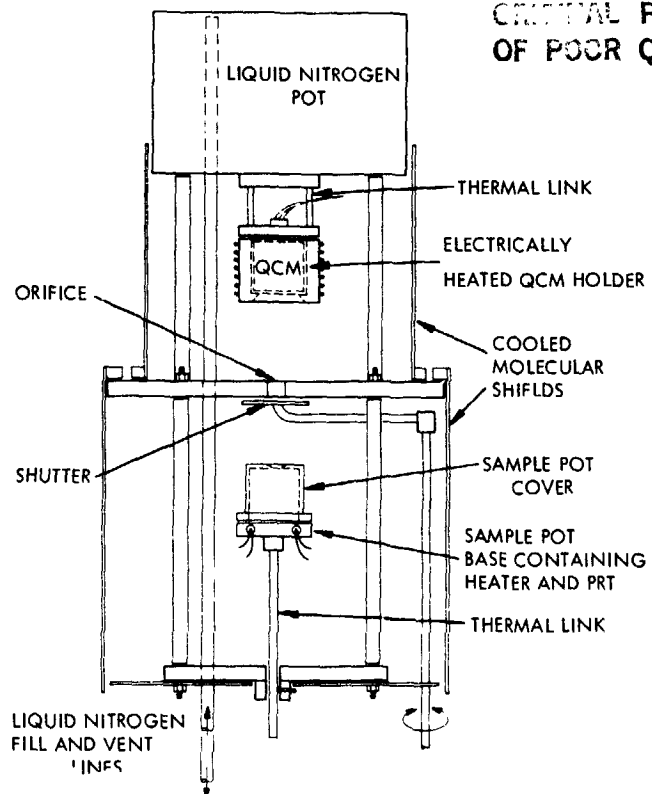


Fig. 3 Thermal Analysis Apparatus

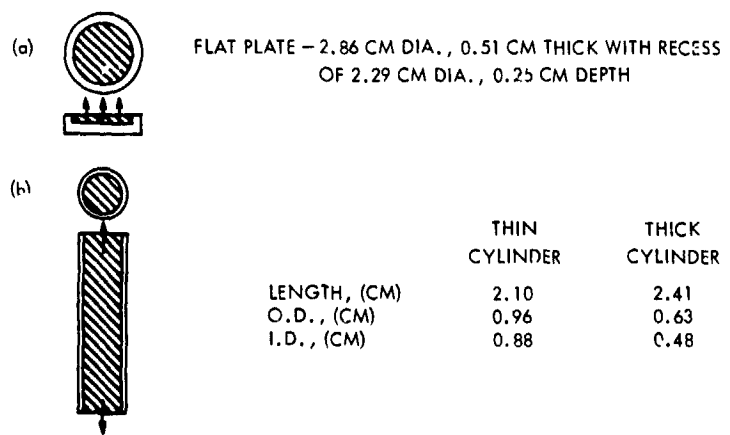


Fig. 4 One-Dimensional Sample Holders

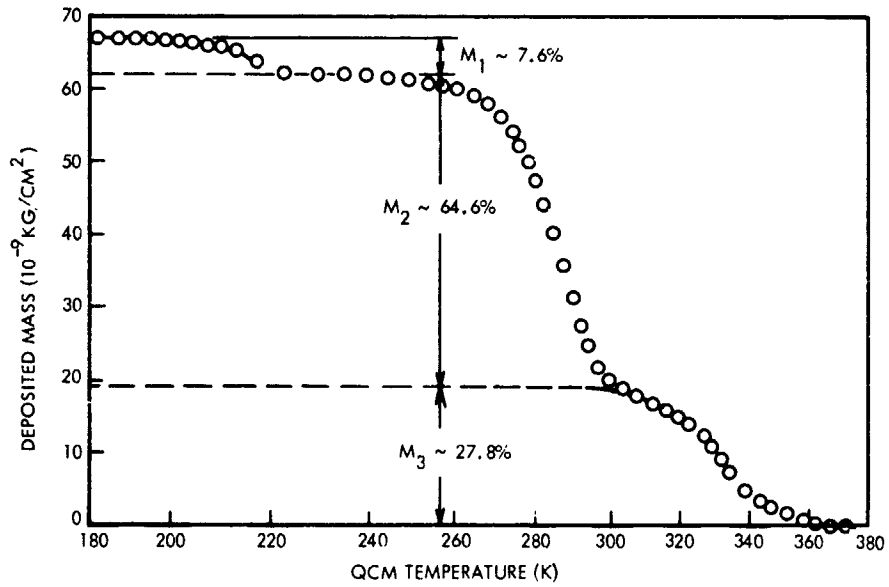


Fig. 5 Reevaporation of RTV 560 Outgas Deposit on QCM - Test 8R

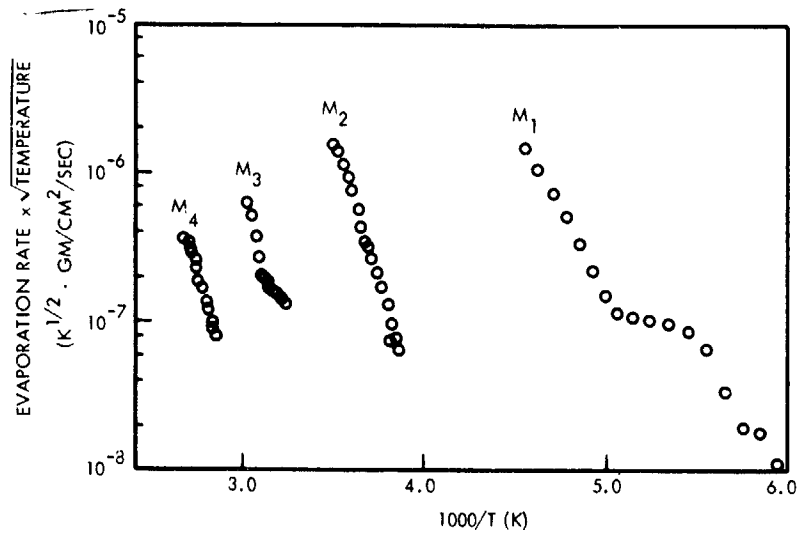


Fig. 6 Evaporation Rate of RTV 560 Outgas Species From the Collector QCM

ORIGINAL PAGE IS  
OF POOR QUALITY

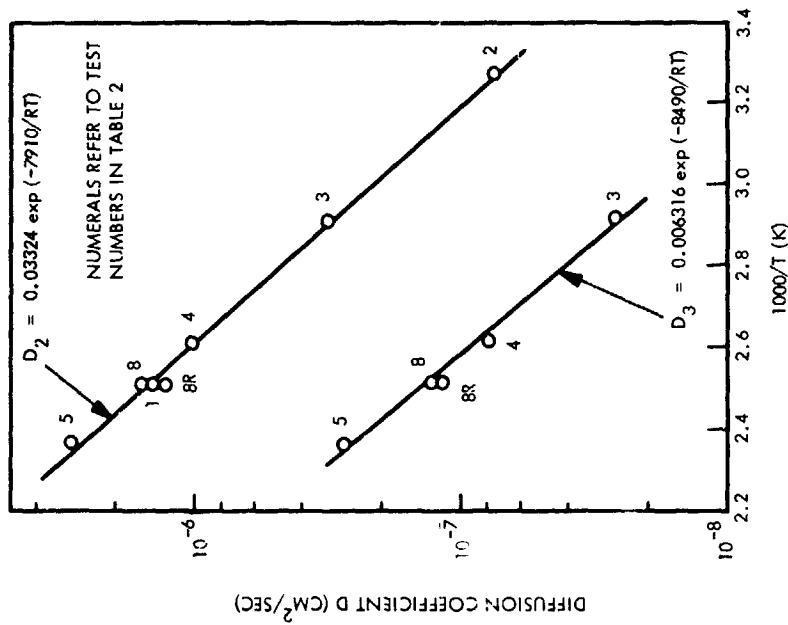


Fig. 8 Diffusion Coefficient of RTV 560  
Outgas Species

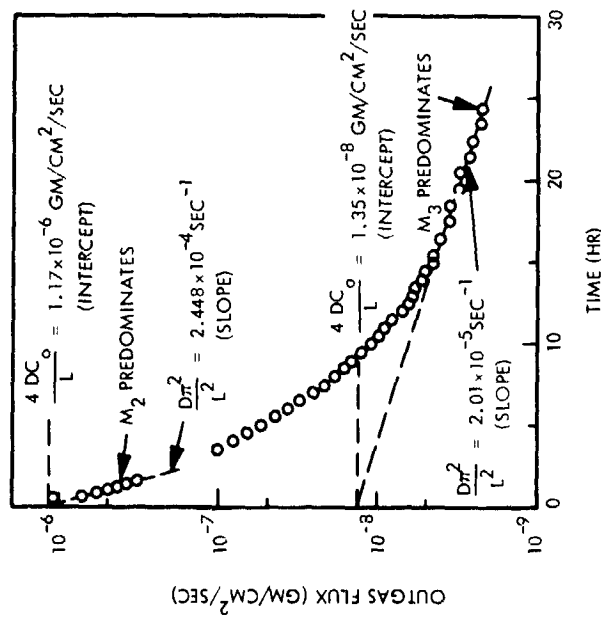


Fig. 7 Determination of  $D$  and  $C_0$  From  
Typical Outgassing Data - Test 8  
Sample Temperature = 398 K,  
Diffusion Length = 0.25 cm

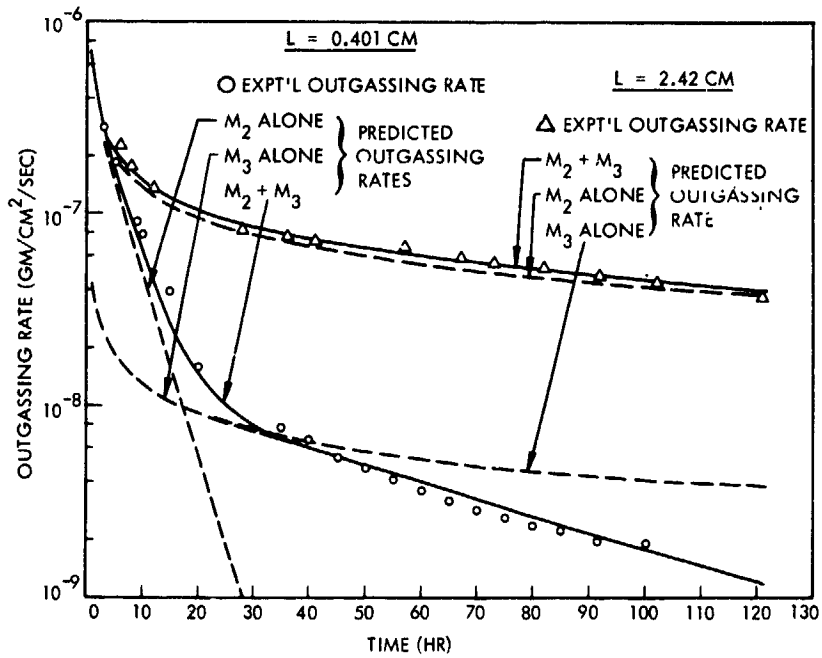


Fig. 9 Comparison of Measured and Predicted RTV 560 Outgas rate and Relative Amounts of  $M_2$  and  $M_3$  at 383 K for Two Diffusive Flow Path Lengths

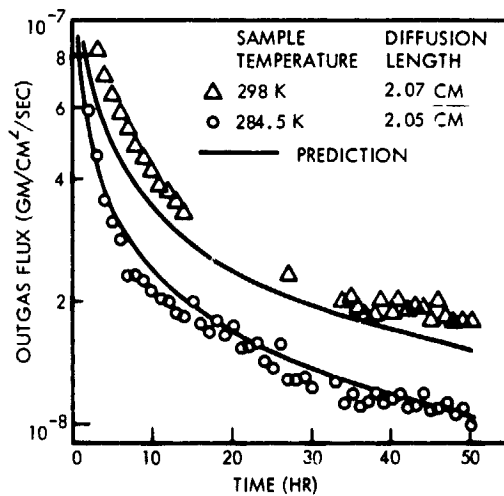


Fig. 10 Comparison of Measured and Predicted Outgassing Rate of RTV 560 at 298 K and 284.5 K